Reduction-Sensitive Dextran Nanogels Aimed for Intracellular Delivery of Antigens

Dandan Li, Neda Kordalivand, Marieke F. Fransen, Ferry Ossendorp, Koen Raemdonck, Tina Vermonden, Wim E. Hennink, and Cornelus F. van Nostrum*

Targeting of antigens to dendritic cells (DCs) to induce strong cellular immune response can be established by loading in a nano-sized carrier and keeping the antigen associated with the particles until they are internalized by DCs. In the present study, a model antigen (ovalbumin, OVA) is immobilized in cationic dextran nanogels via disulfide bonds. These bonds are stable in the extracellular environment but are reduced in the cytosol of DCs due to the presence of glutathione. Reversible immobilization of OVA in the nanogels is demonstrated by the fact that hardly any release of the protein occurred at pH 7 in the absence of glutathione, whereas rapid release of OVA occurs once the nanogels are incubated in buffer with glutathione. Furthermore, these OVA conjugated nanogels show intracellular release of the antigen in DCs and boost the MHC class I antigen presentation, demonstrating the feasibility of this concept for the aimed intracellular antigen delivery.

1. Introduction

Many peptides and proteins have been used as antigens for the generation of antigen-specific immune responses. Protein antigens are in their soluble form usually safe and well tolerated; however, they induce low levels of immune responses because of their poor uptake by antigen presenting cells.[1] A promising strategy to enhance protein and peptide vaccine potency is to incorporate them into particulate carriers.[1d,2] Nanoparticulate delivery systems (e.g., liposomes, polymeric carriers) have been used for vaccination as they offer advantages in many aspects. They protect the antigen against degradation, and encapsulation of antigen in particles results in an increased uptake by dendritic cells (DCs) and delivery of relative large quantities of

antigens into DCs.[3] Moreover, particles enable co-delivery of the antigen and an adjuvant.[3a,4] Overall, these features result in an increased immunogenicity of the antigen. A vaccine delivery vehicle needs to be designed to target the immune system, particularly DCs. It has been shown that the size of vaccine delivery systems is a critical parameter affecting immunogenicity. Small nanoparticles (<200 nm) can after, e.g., subcutaneous administration traffic to the draining lymph nodes where they are then internalized by antigen-presenting cells (APCs), whereas large particles (500–2000 nm) are taken up by local APCs at the injection site. However, large particles are predominantly internalized and digested by local macrophages.[5]

Smaller sized particles (<500 nm), in particular <50 nm, are taken up more efficiently than large particles by DCs and have better ability to promote CD8+ T-cell immunity, which is crucial for immunotherapy against cancer and viral infectious diseases. In contrast, larger particles (>500 nm) tend to present antigens to CD4+ T-cells and induce antibody responses for bacterial infectious diseases.[5d,6] Another important factor to enhance the immune response is keeping the antigen encapsulated or associated with the particles until their internalization by DCs, and it has been shown that low-burst release is crucial for a strong immune activation.[7]

One of the most attractive nanosized delivery systems for proteins is nanogels because of their 1) tunable chemically or physically crosslinked structures, 2) high water content (resulting in good protein/antigen compatibility), and 3) high loading capacity for water-soluble proteins/peptides.[8] Physically crosslinked gels are mechanically weak and prone to rapid dissociation in the body.[9] Therefore, chemically crosslinked nanogels are preferred for drug delivery applications. However, a disadvantage of chemically crosslinked nanogels is the instability of proteins due to exposure to crosslinking agents. This exposure may cause unwanted chemical modification of the protein, or the protein may be grafted to the network, which could lead to incomplete release.[8b,10] To avoid this, post-loading after nanogel fabrication is a good alternative; however, such an approach may suffer from burst or preliminary release before the particles are internalized by cells due to the gel's high water content and often large pore sizes.[11]
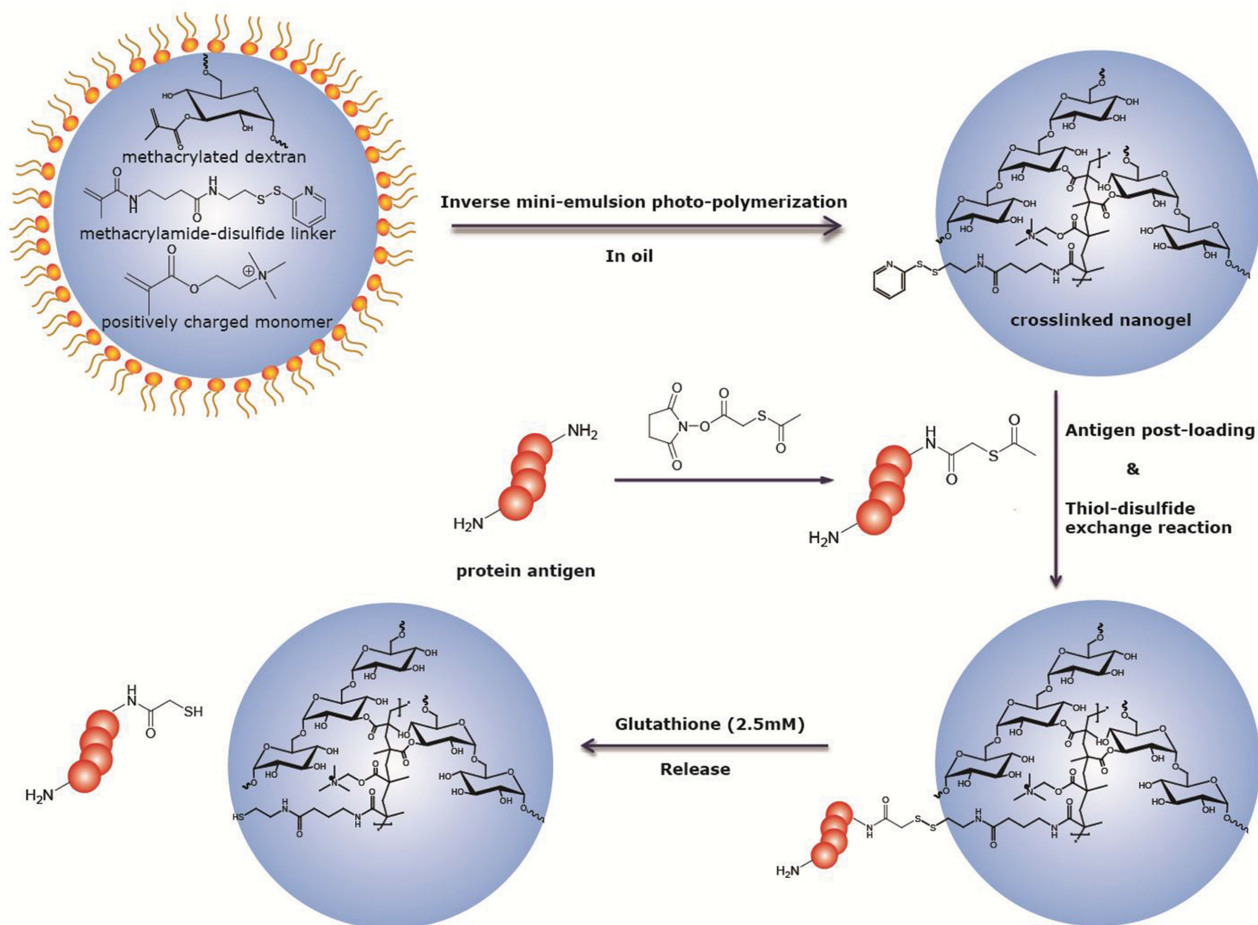
Depending on the pH of the medium, above or below the iso-electric point (pI), a protein is electrostatically charged, so it can be post-loaded into oppositely charged nanogels exploiting electrostatic interactions between protein and particle as the

D. Li, N. Kordalivand, Dr. T. Vermonden,
Prof. W. E. Hennink, Dr. C. F. van Nostrum
Department of Pharmaceutics
Utrecht Institute for Pharmaceutical Sciences
Utrecht University
Universiteitsweg 99, 3584 CG, Utrecht, The Netherlands
E-mail: C.F.vanNostrum@uu.nl
Dr. M. F. Fransen, Prof. F. Ossendorp
Department of Immunohematology and Blood Transfusion
Leiden University Medical Center
Albinusdreef 2, 2333 ZA, Leiden, The Netherlands
Dr. K. Raemdonck
Laboratory of General Biochemistry and Physical Pharmacy
Ghent University
Ottergemsesteenweg 460, 9000 Gent, Belgium

DOI: 10.1002/adfm.201500894

ADVANCED
FUNCTIONAL
MATERIALS
www.afm-journal.de

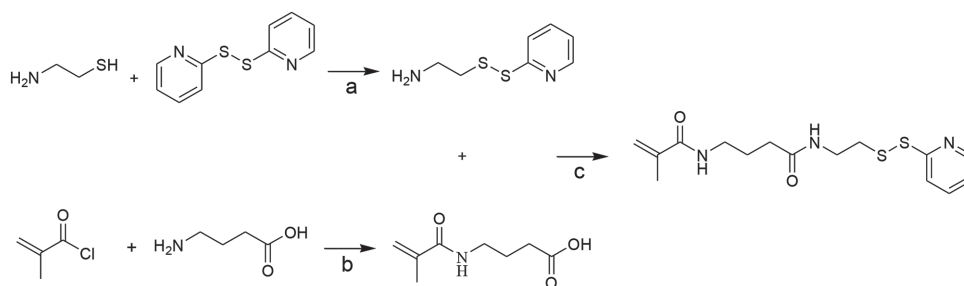Materials
Views
www.MaterialsViews.com

FULL PAPER

Scheme 1. Schematic representation of the preparation of dextran nanogels and loading/triggered release of protein.

driving force, thereby avoiding protein damage during hydrogel formation.[10a,12] In this work, to control the protein release after their uptake by cells, we have designed dextran nanogels in which proteins are reversibly immobilized via disulfide bonds after electrostatically driven post-loading. A designed disulfide-containing linker is used to couple the protein derivatized with succinimidyl S-acetylthioacetate (SATA) groups to the nanogels. This method was recently used by Verheyen et al. with bulk hydrogels and by Matsumoto et al. with nanogels.[13] The disulfide bonds between proteins and nanogels are stable in the extracellular environment but are degraded in the cytosol of cells, because of relatively high intracellular levels of glutathione as compared with the extracellular space,[14] so that triggered release of the loaded antigen can be achieved after their internalization by DCs (**Scheme 1**). This study focuses on developing antigen–nanogel conjugates, using ovalbumin (OVA) as the model protein antigen, which show triggered release of their payload in a reductive environment.

2. Results and Discussion

OVA (43 kDa), due to its pI of 4.9,[15] is negatively charged at pH 7. Therefore, cationic dextran nanogels were prepared by inverse mini-emulsion photo-polymerization of methacrylated dextran (dex-MA),[16] trimethyl aminoethyl methacrylate (TMAEMA), and a pyridyldisulfide-containing methacrylamide monomer (see Scheme 1). Free radical polymerization of the methacrylate groups of dex-MA in the aqueous solution provides a stable hydrogel. Dextran gels have been used as protein delivery systems, and its biocompatibility has been shown previously.[17] The network density of the formed gel can be tuned by the degree of methacrylate substitution (DS, the number of methacrylate groups per 100 saccharide moieties) of dex-MA and/or by its concentration.[18] Introducing TMAEMA, a cationic methacrylate monomer, provides the nanogels with positive charges, whereas the ζ-potential of the nanogel particles depends on the amount of charged monomers per surface area.[19] The charge density of the networks (reflected by the ζ-potential), in turn, influences the absorption behavior of the loaded protein including loading amount and distribution.[12a] A specially designed linker containing a methacrylamide unit and a pyridinedisulfide unit was synthesized (**Scheme 2**). This linker was copolymerized with dex-MA and TMAEMA in the nanogel networks to allow subsequent conjugation with thiolated OVA through a thiol–disulfide exchange reaction so that the modified antigen is chemically linked to the nanogels via disulfide bonds.[13b]

Materials
Views
www.MaterialsViews.com

ADVANCED
FUNCTIONAL
MATERIALS
www.afm-journal.de

FULL PAPER

Scheme 2. Synthesis of *N*-(4-(2-(pyridine-2-yldisulfanyl)ethyl)-amidobutyl) methacrylamide. a) acetic acid, CH$_3$OH, b) NaOH/H$_2$O, HCl, c) EDC, HOBt, TEA, CH$_3$Cl.

2.1. Influence of Network Density and Surface Charge on OVA Loading

We prepared eight dextran nanogel formulations with variable network density and ζ-potential to investigate the effect of dextran DS, dextran concentration, and ζ-potential on the OVA loading in nanogels (**Table 1**). All nanoparticles had a mean particle size around 200 nm with a polydispersity index of ≈0.15 (dynamic light-scattering analysis). The ζ-potential of the nanogels increased with increasing feed of TMAEMA, and neutral nanogels were prepared without charged monomers. The nanogels were incubated with an OVA solution in an HEPES buffer of low ionic strength, and the loading capacity was determined by the UPLC analysis of the remaining protein concentration of the supernatant. OVA was not absorbed by the nanogels without TMAEMA because of the lack of electrostatic attraction between the protein and neutral nanogels. In contrast, all cationic nanogels showed rapid absorption and high loading of OVA. It is remarked that loading efficiency reached up to 97% and was similar for different incubation times (1, 24, and 48 h), demonstrating that OVA could be quantitatively absorbed into the gel network within 1 h. Table 1 also shows that the ζ-potentials of the OVA-loaded nanogels were close to zero (from −5 to +5 mV), demonstrating that the protein neutralized the charge of the nanogels. The maximum loading capacity

for each nanogel formulation depended on the charge density of the empty nanogels and accordingly nanogels with higher ζ-potential had higher maximum loading capacity (Table 1). The properties of the different nanogel formulations only differed in maximum loading capacity, which illustrates that the mesh size of the gel network is big enough to allow OVA molecules penetration regardless of DS and content of dex-MA. The high maximum loading capacity of these nanogels is likely because of their porous structure, which is also observed for the loading capacity of porous silicon dioxide and porous calcium silicate materials.[20] In further experiments, we focused on dextran nanogels prepared using DS 8, 20% w/w dex-MA, and 13 molar ratio of TMAEMA to MA in dex-MA.

2.2. Modification of OVA with SATA

For covalent immobilization of OVA in the gel networks, the antigen was modified with protected thiol functions using SATA[13b] for subsequent coupling with the linker present in the particles. OVA has 20 amine groups in the form of lysine units.[21] Varying numbers of thiol groups were introduced by incubating OVA with SATA at different molar ratios (**Table 2**). It is shown that 12 amine groups were available for modification (TNBS assay), likely because the other eight lysine

Table 1. Characterization of nanogels used in this study. Z-average hydrodynamic diameter (Z_{ave}) and ζ-potential (before and after OVA loading) of nanogels with variable degree of methacrylate substitution of dextran (DS), content of dex-MA, and molar ratio of TMAEMA to MA in dex-MA, and the maximum loading capacity (LC) of OVA for the nanogel formulations. The nanogels were dispersed in HEPES buffer (20×10^{-3} M, pH 7.4). Mean values with corresponding standard deviations are shown ($n = 3$).

DS	Content[a] [w/w]	TMAEMA:MA	Z_{ave} [nm]	ζ-Potential before loading [mV]	Max LC[b] [wt%]	ζ-Potential after max loading [mV]
4	20%	25	203 ± 5	23.0 ± 0.9	74.5 ± 5.5	−3.3 ± 0.7
8	20%	13	186 ± 2	22.4 ± 0.6	75.3 ± 1.9	0.9 ± 0.8
10	20%	10	185 ± 3	22.3 ± 0.3	75.0 ± 3.1	−5.1 ± 0.4
8	25%	13	198 ± 6	22.6 ± 0.4	76.1 ± 1.7	2.2 ± 0.3
8	20%	0	213 ± 8	−0.2 ± 0.1	ND[c]	−0.6 ± 0.1
8	20%	2	193 ± 9	11.6 ± 0.2	39.3 ± 9.5	−3.3 ± 0.2
8	20%	4	180 ± 2	16.3 ± 0.3	60.1 ± 6.2	−5.1 ± 0.4
8	20%	21	207 ± 7	26.2 ± 1.2	80.7 ± 1.6	5.5 ± 0.5

[a]dex-MA/water weight ratio; [b]Maximum loading capacity (loaded OVA/dry nanogels plus loaded OVA weight × 100%) by measuring the OVA remaining in the supernatant of nanogels suspension when incubated the nanogels with a sufficient amount of OVA; [c]Not detectable, no OVA (within the experimental error) was loaded in the neutral nanogels.

Table 2. Number of free NH_2 groups and ATA groups after modification of OVA with zero to six equivalents of SATA (OS_x) determined by the TNBS assay ($n = 3$).

Sample	SATA equivalents/OVA	Free NH_2 groups	ATA groups per OVA
Native	0	11.7 ± 0.2	0
OS_2	2	9.7 ± 0.7	1.9 ± 0.7
OS_4	4	8.9 ± 0.4	2.7 ± 0.4
OS_6	6	8.4 ± 0.0	3.2 ± 0.2

residues are deeply buried in the protein.[21] The number of introduced SATA groups was ≈3 for both OS_4 and OS_6 (OS_x, where x stands for the equivalents of SATA used) in accordance with the fact that three of the lysine residues are localized on the surface of the protein and are therefore most reactive, whereas the other amine groups are less accessible and thus less susceptible for derivatization.[21] The structure of the modified protein was investigated by spectral analysis (**Figure 1**). The UV, circular dichroism and fluorescence spectra of native and modified protein showed no significant differences, which illustrates that neither aggregation nor significant changes in the secondary and tertiary structures occurred. OS_4 with an average of 2.7 SATA modifications was used for further study.

2.3. Preparation of OVA Nanogel Conjugates

Dex-MA nanogels with TMAEMA and different linker contents (linker-containing nanogels, LNG_x, where x stands for the equivalents of linker present in nanogels, i.e., 1–3 linker

to OVA equivalents were investigated) were prepared to investigate the efficiency of chemical immobilization of the modified protein. OVA (15 mg dissolved in a 7.5 mL HEPES buffer) was mixed with the different nanogels (85 mg freeze-dried particles suspended in 42.5 mL HEPES buffer 20×10^{-3} M, pH 7.4) for loading. Subsequently, a deacetylation solution (hydroxylamine and EDTA in HEPES buffer) was added. As a result, SATA-modified proteins were deprotected[22] to allow conjugation of the generated free thiol groups to the linkers in the nanogel networks via a thiol–disulfide exchange reaction. No significant changes in size and ζ-potential of nanogels were observed after OVA loading (**Table 3**), which indicates that no particle aggregation occurred and that the protein was absorbed into the nanoparticles rather than adsorbed on the surface. In this respect, it should be noted that substantial lower OVA loadings were applied (≈10–14%, see Table 3), which explains the minimal change in ζ-potential in contrast to the previous experiments (Table 1), where loading capacities of ≈40–80% were obtained and neutral particles were formed after maximum protein loading. Native OVA that could not be covalently linked to the nanogels because of the absence of free thiol groups was used in control formulations. Loading efficiencies of 98% native OVA in nanogels with and without linkers were obtained after washing with the HEPES buffer (Table 3). This table also shows that when these nanogels were washed with buffer of higher ionic strength (PBS), almost quantitative desorption of the loaded native protein occurred. Also, quantitative loading of the modified OVA in the nanogels occurred. Importantly, after deprotection of the SATA groups (addition of hydroxylamine and EDTA in the HEPES buffer) to allow reaction of the formed thiolated protein with the linker, only 28% of the loaded protein was
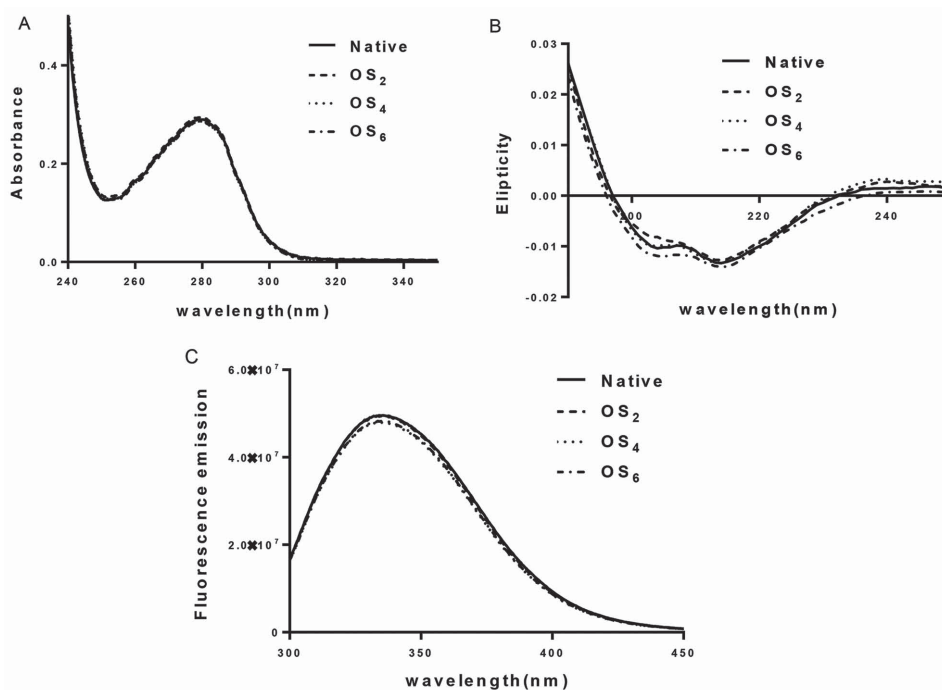
Figure 1. UV–vis spectra A), far-UV CD spectra B), and fluorescence emission spectra C) of SATA-modified ova samples (ratio SATA/OVA = 2, 4, and 6). Spectra (average of 3) were taken of OVA samples at a concentration of 0.5 (UV), 0.25 (CD), and 0.1 (FS) mg mL^{-1} in PBS (pH 7.4).

Table 3. Characterization of OVA-loaded nanogels. Z-average hydrodynamic diameter (Z_{ave}), ζ-potential, loading capacity (LC), and loading efficiency (LE) of OVA-loaded nanogels. The nanogels were dispersed in HEPES buffer (20×10^{-3} M, pH 7.4). Mean values with corresponding standard deviations are shown ($n = 3$).

Nanogels–OVA	Z_{ave}[a)] before loading [nm]	ζ-potential before loading [mV]	LC[b)] washing with HEPES [wt%]	LC[b)] washing with PBS [wt%]	LE[c)] [%]	Z_{ave}[a)] after loading [nm]	ζ-Potential after loading [mV]
LNG$_0$–Native	192 ± 8	23.7 ± 0.6	14.6 ± 0.1	1.2 ± 0.1	97.4 ± 0.6	189 ± 9	22.1 ± 0.6
LNG$_3$– Native	194 ± 7	23.4 ± 0.4	14.7 ± 0.0	1.3 ± 0.1	98.1 ± 0.1	208 ± 6	21.6 ± 0.1
LNG$_1$–OS$_4$	186 ± 2	23.7 ± 0.3	14.6 ± 0.1	10.6 ± 0.2	70.9 ± 1.1	193 ± 3	23.2 ± 0.7
LNG$_2$–OS$_4$	198 ± 5	22.4 ± 1.2	14.5 ± 0.0	10.7 ± 0.1	71.7 ± 0.7	202 ± 2	22.3 ± 0.2
LNG$_3$–OS$_4$	194 ± 7	23.4 ± 0.4	14.7 ± 0.0	10.8 ± 0.1	72.1 ± 0.5	199 ± 1	23.2 ± 0.5

[a)]Polydispersity index (PDI) was <0.15 for all formulations; [b)]Loading capacity (loaded OVA/dry nanogels plus loaded OVA weight × 100%); [c)]Loading efficiency (loaded OVA in nanogels/feed OVA weight × 100%). Loading efficiency for the native OVA is the numbers after washing with HEPES buffer, and for the modified OVA is the numbers after washing with PBS.

desorbed after washing with PBS. This strongly demonstrates that the protein was indeed covalently linked to the hydrogel network. No significant differences between the loading efficiencies of the three nanogels with different linker contents were observed. For LNG$_1$, an approximately equivalent number of protein molecules and linker units in the nanogels was present, whereas for LNG$_2$ and LNG$_3$, a twofold and threefold excess of linker units was used, respectively. Since OS$_4$ has around three SATA groups per molecule (Table 2), the SATA/linker molar ratios for these formulations were 3/1, 3/2, and 1/1. By measuring the 2-mercaptopyridine released due to the thiol–disulfide exchange reaction, the percentage of reacted linkers was determined. The linker units present in LNG1 reacted quantitatively with the modified protein, whereas 87% and 78% were converted for LNG$_2$ and LNG$_3$, respectively.

2.4. In Vitro OVA Release from OVA-Loaded Dextran Nanogels

Figure 2 shows that more than 90% of the native OVA desorbed when the gels were dispersed in a buffer of physiological
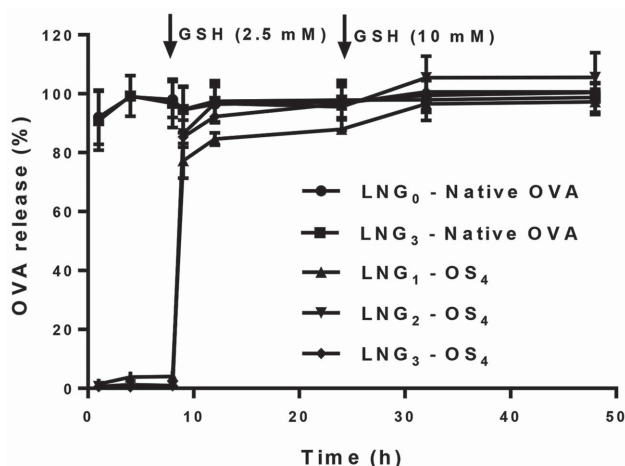
ionic strength (PBS, pH 7.4, 37 °C). The ionic strength of PBS (167.2×10^{-3} M) is much higher than that of the HEPES buffer (20×10^{-3} M, which was used for gel preparation and OVA loading), so the release of native OVA was mediated only by increase of the ionic strength of the medium. The nanogels in which modified OVA was immobilized showed a release of very limited amount of protein during 8 h in PBS (<1% of the loading for LNG$_2$ and LNG$_3$, <5% for LNG$_1$), demonstrating that modified OVA was indeed stably covalently linked to the particles. Importantly, after addition of glutathione to a final concentration that corresponds with intracellular levels (2.5×10^{-3} M),[14a] more than 80% of the covalently bound OVA was released within 1 h as a consequence of the reduction of the disulfide bridges. After 24 h, glutathione was added to a final concentration of 10×10^{-3} M, causing further release of the remaining 5–10% of protein that was still in the gels (Figure 2).

2.5. Confocal Images of Distribution, Penetration, and Release of OVA Dextran Microgels

To visualize the distribution of OVA in dextran gels and release behavior of OVA by fluorescence microscopy, experiments were carried out using FITC-labeled OVA. Because nanogels are very small for microscopy, neutral and cationic microgels instead of nanogels, with similar network and charge densities, were prepared using a dextran/PEG water-in-water emulsion polymerization method (**Table 4**).[23] The microparticles had mean sizes of around 4 µm, and the maximum loading capacities were similar to those of the corresponding nanogels. The microgels were incubated with FITC-labeled OVA for 2 h to obtain OVA-loaded microgels with loading capacities of 15 wt%. The samples were analyzed by confocal laser scanning microscopy (CLSM). CLSM images demonstrated that no fluorescence could be detected in the neutral particles that were immersed in an FITC-OVA solution (**Figure 3**A). In contrast, FITC-OVA was evenly distributed in the different cationic microgels (Figure 3C,D), suggesting that the pore sizes in the different gels are big enough to allow absorption of the protein into the particles.[18b]

CLSM images were recorded in time (1 frame/30 s) to visualize the process of OVA penetration into dextran microgels in the HEPES buffer (**Figure 4**A). After addition of the FITC-OVA

Figure 2. OVA release from dextran nanogels in PBS pH 7.4 at 37 °C; glutathione was added to 2.5×10^{-3} M final concentration at 8 h and to 10×10^{-3} M at 24 h. OVA release was measured by UPLC as described in the Supporting Information.

**ADVANCED
FUNCTIONAL
MATERIALS**
www.afm-journal.de

*Materials
Views*
www.MaterialsViews.com

Table 4. Size, ζ-potential and the maximum OVA loading capacity of microgels ($n = 3$).

DS	Content [w/w]	TMAEMA: MA	$d^{a)}$ [µm]	ζ-Potential before loading [mV]	Max LC$^{b)}$ [wt%]	ζ-Potential after max loading [mV]
4	20%	25	2.89 ± 1.58	21.8 ± 0.3	78.4 ± 8.6	2.5 ± 0.4
8	20%	13	3.21 ± 1.76	21.2 ± 0.6	74.0 ± 2.1	−0.6 ± 0.5
10	20%	10	2.64 ± 1.12	21.3 ± 0.7	77.2 ± 5.4	2.8 ± 0.2
8	25%	13	4.38 ± 3.26	22.3 ± 0.2	75.0 ± 0.1	−0.7 ± 0.8
8	20%	0	4.38 ± 2.98	−1.1 ± 0.2	ND$^{c)}$	−3.6 ± 0.8
8	20%	2	2.45 ± 1.35	11.1 ± 0.7	33.8 ± 3.8	−1.4 ± 0.7
8	20%	4	4.07 ± 2.68	16.1 ± 0.4	55.7 ± 9.3	−3.8 ± 0.2
8	20%	21	3.25 ± 1.83	25.4 ± 0.3	80.0 ± 4.4	1.2 ± 0.7

a)Number mean diameter; b)Maximum loading capacity (loaded OVA/dry microgels plus loaded OVA weight × 100%); c)Not detectable, no OVA was detected in the neutral microgels.

solution to a microgel suspension, fluorescence was already detected in the particles after 30 s. The fluorescence increased in time (not shown) and reached a maximum at 5 min indicating that the protein was quantitatively absorbed by the particles. It is further noted that fluorescence was homogenously distributed in the particles, demonstrating that the pores in the hydrogel network are bigger than the hydrodynamic diameter of the protein. Since in this case FITC-OVA was not covalently linked to the network of particles, addition of PBS buffer led to release of OVA within minutes (Figure 4B).

FITC-OVA was also modified with SATA and conjugated to microgel particles containing the pyridyldisulfide linker. The release behavior was again visualized by CLSM (**Figure 5**). After addition of PBS to the microgel suspension, no significant decrease in fluorescence intensity was observed demonstrating that the protein remained immobilized in the hydrogel network. However, after addition of glutathione, the fluorescence in the particles substantially dropped within 1 min indicating extremely fast release due to cleavage of the disulfide bonds.

2.6. Intracellular Release of OVA from Nanogels in D1 Cells (DCs)

To show the intracellular release of the conjugated OVA, OVA-loaded nanogels were double labeled. The nanogels were labeled with Alexa Fluor 488 (AF488), whereas OVA was labeled with Alexa Fluor 647 (AF647). Confocal images were taken after incubation of the OVA nanogels with D1 cells for 24 h. Cells incubated with OVA conjugate nanogels showed colocalization of the labels on the surface of the cells (yellow, overlap of green and red, in **Figure 6**A). On the other hand, within the cells only empty nanogels (green) were observed, which indicates that the conjugated OVA was released from the nanogels upon their internalization. In contrast, Figure 6B shows only green spots, indicating that the nonconjugated OVA nanogels released the protein before they were taken up by cells. It should be noted that no signal was observed for released AF674-OVA likely because the released OVA is diluted in the cells below detection level. However, in some cases, the released OVA had a sufficient high concentration in the cytosol, and the released OVA could be visualized (see Figure S1 in Supporting Information). As controls, free OVA and empty neutral nanogels were not internalized by D1 cells after 24 h incubation (Figure 6C,D).

2.7. MHC Class I Antigen Presentation

The ability of OVA conjugated particles for antigen presentation by DCs and subsequent activation of CD8$^+$ T cells was tested in vitro. An MHC class I antigen presentation assay[24] was performed with DC incubated with both OVA nanogels and microgels (**Table 5**) and compared with soluble OVA and H-2Kb-restricted OVA class I epitope SIINFEKL (the OVA
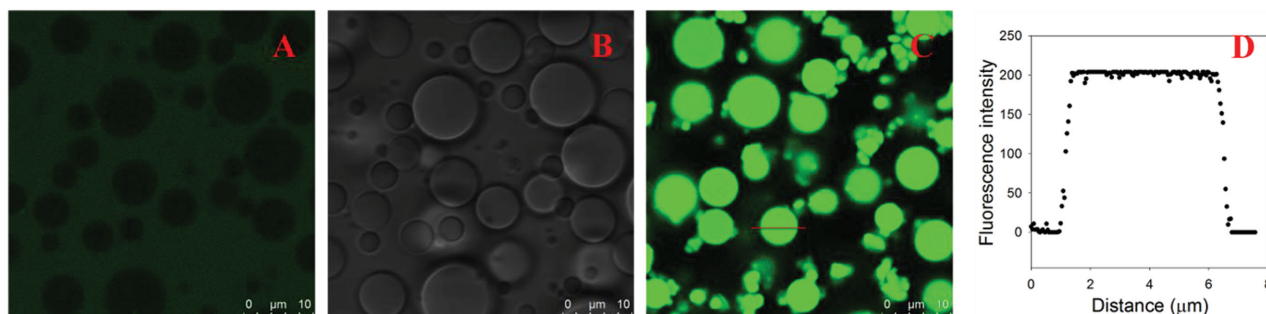
Figure 3. A) CLSM image and B) differential interference contrast image of neutral dextran microgels in FITC-OVA solution. C) CLSM image of OVA-loaded cationic dextran microgels (DS 8, 20% w/w, 13 molar ratio TMAEMA, and 15 wt% loading of OVA). D) Corresponding fluorescence intensity profile, plotted along a microgel cross-section indicated by the line in image (C).
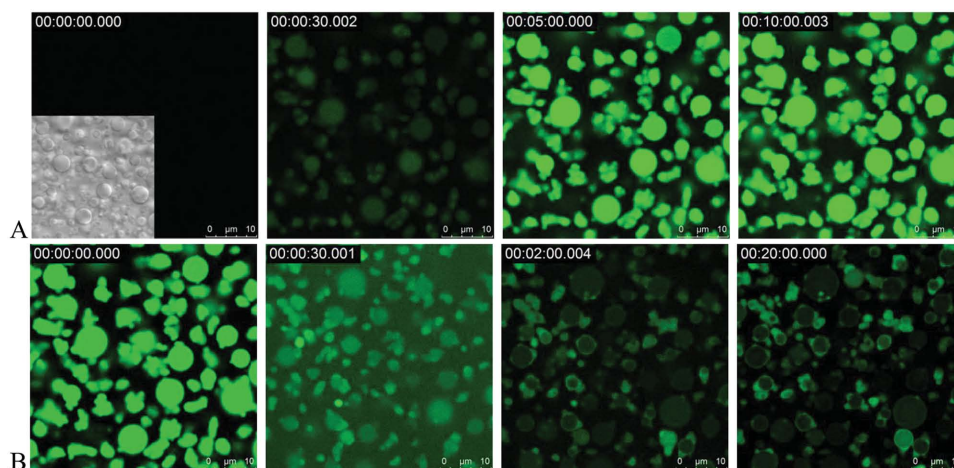
Figure 4. A) Confocal snapshots of cationic dex-MA microgels (DS 8, 20% w/w, 13 molar ratio TMAEMA) dispersed in an FITC-OVA solution in 20×10^{-3} M HEPES pH 7.4 at ambient temperature. The images shown (upper panels from left to right) were taken at 0, 30, 300, and 600 s, whereas FITC-OVA was added at 10 s. B) Confocal snapshots of FITC-OVA-loaded dex-MA microgels (DS 8.0, 20% w/w, 13 molar ratio TMAEMA) upon addition of PBS at ambient temperature. The images shown (lower panels from left to right) were taken at 0, 30, 120, and 1200 s while PBS was added at 10 s.

fragment that is presented by the class I MHC molecule.[25] D1 cells were incubated for 24 h with titrated amounts of OVA and particles before CD8+ T cell hybridoma B3Z cells were added, followed by 24 h incubation at 37 °C. The hybridoma B3Z cells produce β-galactosidase after activation by DCs that present SIINFEKL, thus allowing measurement of MHC class I antigen presentation by a colorimetric assay using chlorophenol red-β-D-galactopyranoside (CPRG). As shown in **Figure 7**, D1 cells incubated with soluble OVA or a mixture of OVA and empty neutral nanogels were not able to activate T cells, which indicates that free OVA is inefficiently taken up by DCs and/or processed in the MHC class I pathway. In contrast, the OVA nanogel/microgel conjugates showed significantly (a factor of 2.5) higher extent of T cell activation compared with their nonconjugated counterparts, and we showed that OVA nanogels were more efficient in stimulating B3Z CD8+ T cells than microgels. This is presumably because of the smaller size and better uptake of the OVA nanogels by D1 cell.[5a,c,6] It should be noted that for positively charged nanogels and microgels, the highest concentration of OVA led to lower T cell activation than lower concentrations likely due to cytotoxicity (**Figure 8**). Therefore, we also included in this study a nanogel
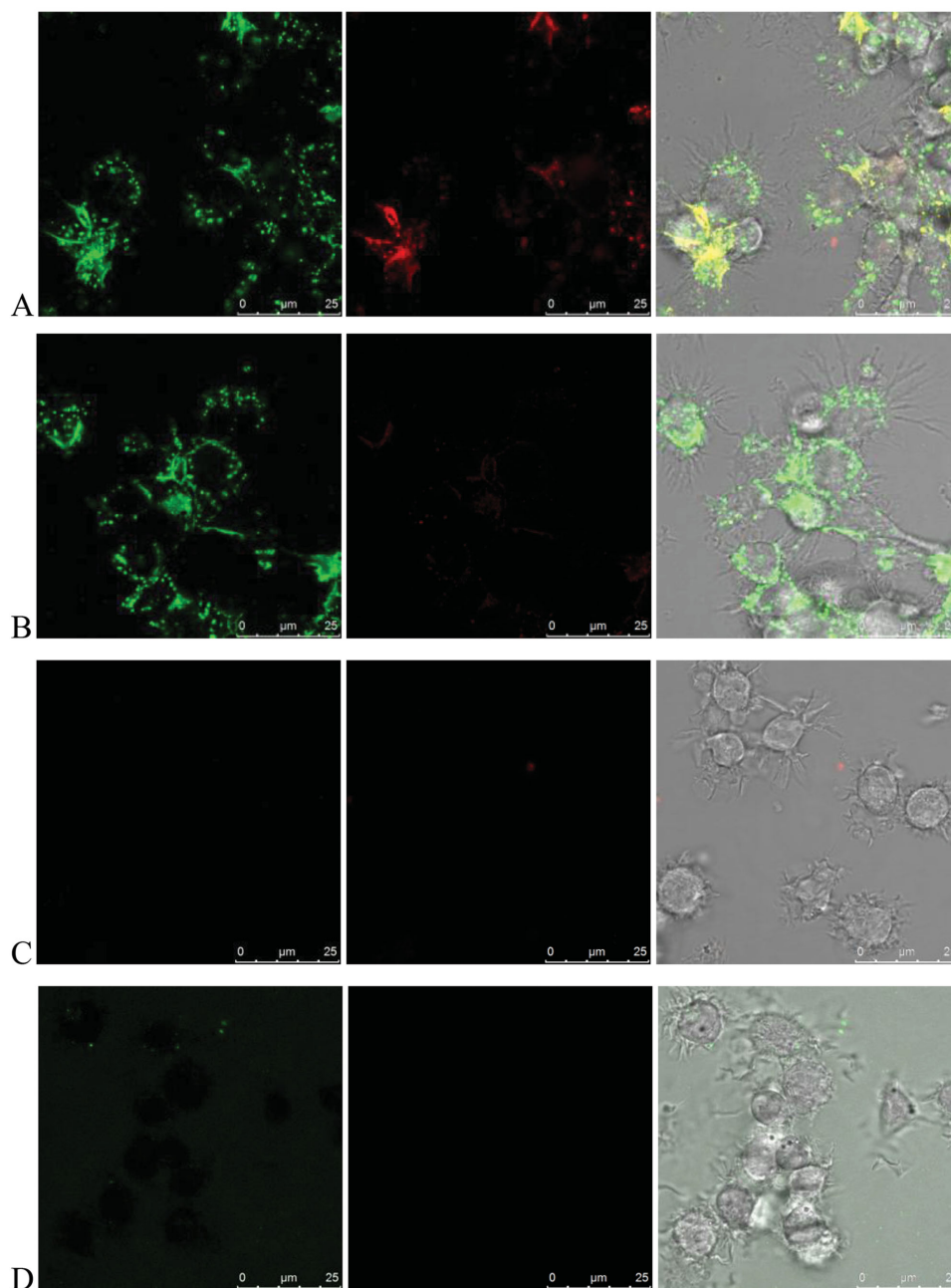
preparation with a lower excess of cationic charge (ζ-potential of 12 mV). The extent of T cell activation stimulated by these lowly charged OVA conjugated nanogels did show dose dependency, meaning that in the dose range investigated the lowly charged nanogels have a good cytocompatibility and are, therefore, the preferred formulations. The improved MHC class I antigen presentation by OVA-conjugated nanogels demonstrates that a high amount of OVA was delivered and released into the D1 cells and the nanogels facilitated processing and presentation of extracellular antigens in MHC class I molecules to CD8+ T cells (cross-presentation).

3. Conclusion

In conclusion, we have developed dextran nanogels in which a model antigen (OVA) was covalently linked via disulfide bonds. An important advantage of this system is that the protein remained stably entrapped in a nonreducing environment; however, triggered and rapid release in the presence of glutathione occurred. Furthermore, high loading capacities were obtained, which enables delivery of large quantities
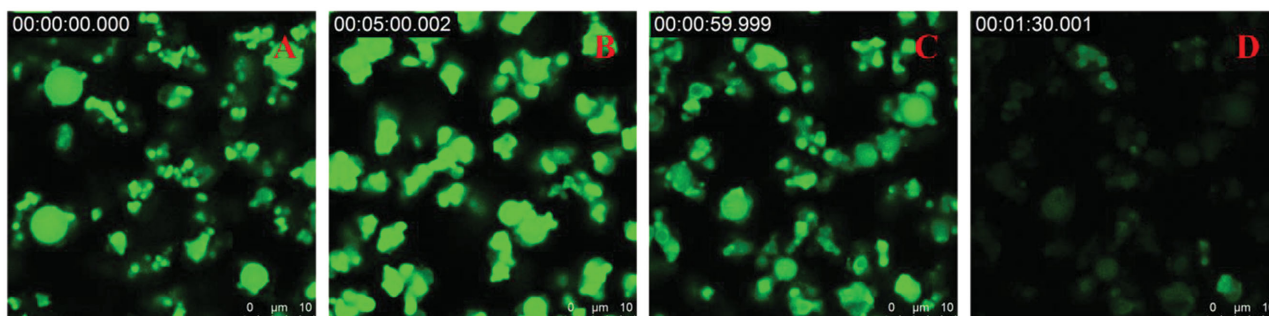
Figure 5. A,B) Confocal snapshots of FITC-OVA microgels conjugate at ambient temperature. The images shown were taken at 0 and 600 s whereas PBS was added at 10 s. After 5 min incubation in PBS, the imaging was stopped. C,D) New snapshots of FITC-OVA microgels conjugate dispersed in PBS were started and the images shown were taken at 60 and 90 s whereas glutathione (2.5×10^{-3} M) was added at 40 s.

ADVANCED
FUNCTIONAL
MATERIALS

www.afm-journal.de

Materials
Views

www.MaterialsViews.com

Figure 6. Intracellular release of OVA nanogels was studied by confocal microscopy. The nanogels were labeled with AF488 (green), and AF647 (red) labeled OVA was loaded. D1 dendritic cells were incubated with nanogels for 24 h at 37 °C and the images were taken (left: AF 488-nanogels, middle: AF647-OVA, right: merged image of AF488, AF647 and differential interference contrast image). A) Conjugated OVA nanogels, B) nonconjugated OVA nanogels, C) free OVA, and D) neutral nanogels.

of antigen into DCs to maximize exposure of antigen to the immune system. Finally, these particles show intracellular delivery and release of antigens in DCs and efficiently facilitate the MHC class I antigen cross-presentation. This technology can be broadly applied for encapsulating a wide variety of therapeutics that can be modified with a thiol group, thus making it a promising system for intracellular antigen delivery.

4. Experimental Section

Synthesis of N-(4-(2-(Pyridine-2-yldisulfanyl)ethyl)-amidobutyl) methacrylamide: a) Synthesis of pyridine dithioethylamine hydrochloride: methanol (25 mL) was used to dissolve 2,2′-dithiodipyridine (11.0 g, 50 mmol, Sigma) and mixed glacial acetic acid (2 mL, 35.0 mmol) under nitrogen. Cysteamine hydrochloride (2.86 g, 25.0 mmol, Sigma) dissolved in 20 mL methanol was added slowly to the mixture. The reaction mixture was stirred for 48 h at room temperature. The product was precipitated by dropping the reaction mixture into cold

www.MaterialsViews.com

ADVANCED
FUNCTIONAL
MATERIALS
www.afm-journal.de

FULL PAPER

Table 5. Z-average hydrodynamic diameter (Z_{ave}), polydispersity index (PDI), ζ-potential, and loading capacity (LC) of OVA-loaded particles used in antigen presentation studies.

| OVA-loaded particles	Z_{ave}	PDI	ζ-potential [mV]	LC [wt%]
Nonconjugated OVA nanogels	198 ± 6 nm	0.13 ± 0.02	20.6 ± 0.3	11.1 ± 0.1
Conjugated OVA nanogels	207 ± 3 nm	0.07 ± 0.01	20.6 ± 0.7	11.7 ± 0.1
Conjugated OVA nanogels, lowly charged	225 ± 7 nm	0.12 ± 0.04	12.2 ± 0.6	10.5 ± 0.3
Nonconjugated OVA microgels	2.75 ± 1.72 μm		20.8 ± 0.7	14.0 ± 0.1
Conjugated OVA microgels	2.54 ± 2.19 μm		22.3 ± 0.2	14.3 ± 0.2
Conjugated OVA microgels, bigger size	8.55 ± 8.33 μm		22.4 ± 0.1	14.2 ± 0.1

ether (200 mL), and purified by redissolving in methanol (15 mL) and precipitating in cold ether (200 mL) until a white powder (4.54 g, 82% yield) was obtained. b) Synthesis of *N*-methacryloyl aminobutanoic acid: aminobutyric acid (8.2 g, 80 mmol, Sigma) and NaOH (6.4 g, 160 mmol) were dissolved in water (15 mL) at 0 °C. A spatula tip of hydroquinone monomethylether was added to the mixture to prevent polymerization. Next, methacryloyl chloride (8.4 g, 80 mmol, Sigma) was slowly added to the mixture that was subsequently stirred overnight. HCl was added after the reaction to adjust to pH 3. The reaction mixture was extracted three times with chloroform. The combined organic layers were washed with water, dried with MgSO$_4$, and filtered. The filtrate was concentrated by rotary evaporation to obtain the product (11.1 g, 81% yield) as a colorless oil. c) *N*-(4-(2-(pyridine-2-yldisulfanyl)ethyl)-amidobutyl) methacrylamide: pyridine dithioethylamine hydrochloride (4.0 g, 18 mmol), *N*-methacryloyl aminobutanoic acid (5.8 g, 36 mmol), HoBt (5.8 g, 43 mmol), and TEA (3.5 mL, 26 mmol) were dissolved in dry DCM (70 mL) under nitrogen. The reaction mixture was cooled on ice and EDC (8.1 g, 43 mmol) was subsequently added to the mixture. The reaction mixture was allowed to warm to room temperature and stirred for 24 h. The reaction mixture was washed with 5% NaHCO$_3$ and brine. Most of the solvent was evaporated and the remaining was purified on a silica gel column (ethyl acetate/acetone, 3:2 (v/v), R_f: 0.37). The product (3.4 g, 55% yield) was obtained as a white powder (purity: 99.5%, which is determined by HPLC).

Modification of OVA with Succinimidyl S-Acetylthioacetate: SATA (10 mg mL^{-1}, dissolved in dry DMSO, Sigma) was added to OVA solutions (2.5 mg mL^{-1}, dissolved in PBS, Serva Electrophoresis GmbH) with molar ratios of 2:1, 4:1, and 6:1. The mixtures were incubated for 30 min at room temperature. The modified OVA was dialyzed against distilled water for 24 h at 4 °C. The number of modified lysine residues was determined by using the TNBS assay.

Spectral Analysis of SATA Modified OVA: (a) UV–vis absorption spectra of 0.5 mg mL^{-1} native and modified OVA in PBS buffer were measured in the range of 250–350 nm by a Shimadzu UV-2450 UV–vis spectrophotometer (Shimadzu Corporation, Kyoto, Japan). (b) Far UV-CD spectra of 0.25 mg mL^{-1} native and modified OVA in PBS buffer were recorded from 250 to 195 nm by a dual-beam DSM 1000 CD spectropolarimeter (On-Line Instruments Systems, Bogart, GA) using cuvettes with a path length of 0.20 mm. (c) Fluorescence measurements were carried out with Horiba Fluorolog fluorometer FL3-21 (Horiba Jobin Yvon, Longjumeau Cedex, France). The excitation wavelength was set at 280 nm and the emission spectra were recorded in the range of 300–350 nm. Native and modified OVA were measured at a concentration of 0.1 mg mL^{-1} in PBS at pH 7.4.

Preparation and Characterization of Empty Dextran Nanogels: Dex-MA (120 mg) was dissolved in distilled water without or with a known amount of the cationic methacrylate monomer TMAEMA (e.g., 160 μL TMAEMA solution for 13 molar ratio of TMAEMA to dextran formulation, Sigma) and without or with linker solution (e.g., for LNG$_3$ formulation: 40 μL linker solution of 120 mg mL^{-1} in 50:50 v/v DMSO/H$_2$O) to a final volume of 360 μL. Subsequently, photoinitiator solution (irgacure 2959, 10 mg mL^{-1} in water, 120 μL, Ciba) was added. This dextran solution was emulsified in the external phase (light mineral oil (Sigma), containing 10% v/v ABIL EM 90 surfactant (Goldschmidt)) by vortexing and ultrasonication for 2 min (cycle-1, amplitude 60%, Labsonic Tip Sonifier, Braun, Melsungen, Germany). The emulsified nanodroplets were polymerized by UV irradiation (15 min, Bluepoint UV source, Hönle UV technology, Germany). The crosslinked nanoparticles were purified by five times washing with acetone/hexane (50:50 v/v), and then rehydrated and lyophilized (yield: ≈90%). The average size and ζ-potential of the nanogels were measured using DLS (Malvern ALV/CGS-3 Goniometer, Malvern Instruments, Malvern, UK) and Zetasizer (Zetasizer Nano, Malvern Instruments, USA). The linker content of nanogels was determined by incubating the nanogels (10 mg) with DTT (5 × 10^{-3} M in PBS, 1 mL) and then by measuring 2-mercaptopyridine in the supernatant that was cleaved and released from the linker present in nanogels. 2-Mercaptopyridine was determined by HPLC (Waters, USA) equipped with a Sunfire C18 column 5 μm (4.6 × 150 mm) (Waters) and tunable ultraviolet/visible light detector (Waters) set at 280 nm. A gradient elution was
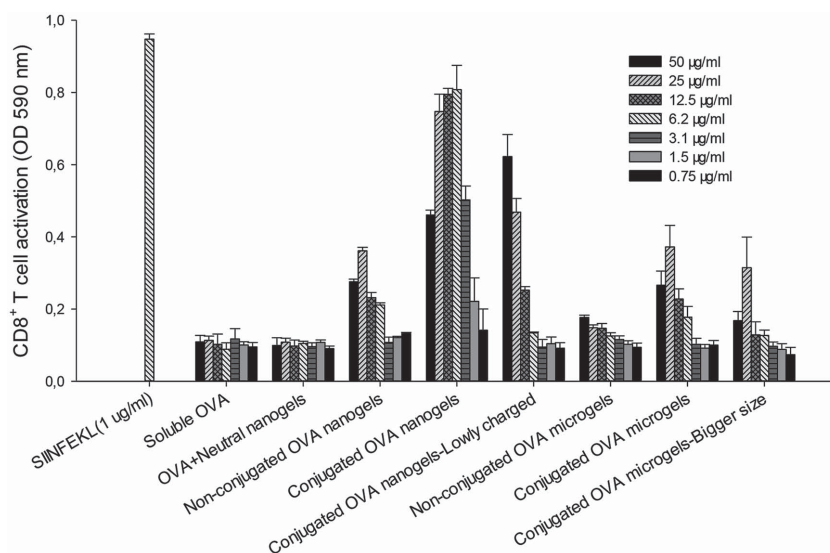
Figure 7. CD8$^+$ T cell activation of SIINFEKL-specific CD8$^+$ T cells (B3Z) after co-culturing with DCs. DCs were incubated with SIINFEKL (1 μg mL^{-1}, positive control), soluble OVA, soluble OVA mixed with empty neutral nanogels and various OVA-loaded particles (Table 5) for 24 h with titrated amounts of OVA. Data are shown as means of triplicate measurement ± SD. Representative results from one of three experiments are shown.
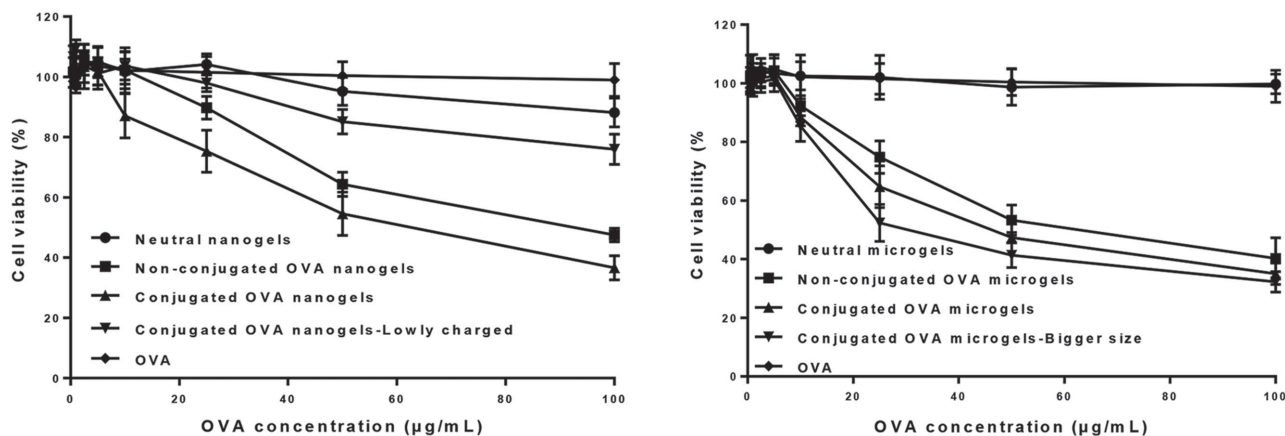
Figure 8. Viability of D1 cells, incubated for 24 h with soluble OVA, neutral particles and OVA-loaded particles. The colorimetric reading at 490 nm of nontreated cells was set at 100% and all data are shown as mean ± SD ($n = 4$). Representative results from one of three experiments are shown. The neutral nano/microgels do not contain OVA. The concentrations of particles were equal to those of the OVA-loaded nano/microgels.

applied with mobile phase A being a 10% ACN aqueous solution and mobile phase B being 100% ACN. The gradient was from 100% to 60% mobile phase A over a period of 6 min with a flow rate of 1 mL min^{-1}. The 2-mercaptopyridine calibration curve was linear between 1 and 50 µg mL^{-1}.

Preparation and Characterization of Empty Dextran Microgels: PEG (2.77 g), dex-MA (81.6 mg), known amounts of TMAEMA, and linker solutions (500 mg mL^{-1} in DMSO) were added in HEPES buffer (100 × 10^{-3} M pH 7.4) to final 20 g in a 50 mL tube. The mixture was flushed with nitrogen and vortexed for 2 min at maximum intensity. A water-in-water emulsion was formed and then allowed to stabilize for 10 min. Next, a sodium bisulfite solution (720 µL, 20 mg mL^{-1}) and a KPS solution (720 µL, 50 mg mL^{-1}) were added to the mixture. The formed droplets were allowed to crosslink overnight at room temperature. The polymerized particles were purified by three times washing with water and then lyophilized (yield: ≈80%). The particle size distribution and ζ-potential of the microgels were measured using AccuSizer (PSS-Nicomp, Sta Barbara, CA, USA) and Zetasizer (see the above), respectively. The linker content was determined by HPLC, as described in the previous paragraph.

Determination of Loading Capacity and Loading Efficiency of the Gels: The concentration of the OVA solution was fixed at 2 mg mL^{-1} in 20 × 10^{-3} M HEPES buffer pH 7.4. Different nanogels/microgels suspensions (0.5 mg mL^{-1} in 20 × 10^{-3} M HEPES buffer, pH 7.4) were mixed with this OVA solution at a volume ratio of 1:1. Samples were taken at different time points (1, 24, and 48 h), and the particles were centrifuged at 15 000 rmp for 60 min (nanogels) or 30 min (microgels). The concentration of OVA in the supernatant was measured by BCA protein assay (25–2000 µg mL^{-1}). Loading capacity (LC) and loading efficiency (LE) were calculated as follows: LC = loaded OVA/dry nanogels plus loaded OVA weight × 100% and LE = loaded OVA in particles/feed OVA weight × 100%.

Preparation and Characterization of 15 wt% OVA-Loaded Nanogels/ Microgels: OVA solution (native or SATA modified, FITC-labeled or nonlabeled, 2 mg mL^{-1}, 7.5 mL) was mixed with particles suspension (without or with varying amount of linker, 2 mg mL^{-1}, 42.5 mL) in HEPES buffer (20 × 10^{-3} M, pH 7.4). The mixture was incubated at room temperature for 1 h to allow OVA loading into the particles. Subsequently, a deacetylation solution (1.72 g hydroxylamine 50% water solution, 0.365 g EDTA in 50 mL HEPES buffer, 5 mL) was added and the mixture was incubated for 2 h. The OVA-loaded particles were collected and purified by multiple washing and centrifugation steps (thrice with PBS for modified OVA or with HEPES buffer for native OVA, 60 min, 15 000 rpm), and then lyophilized (yield: ≈70% for nanogels and ≈80% for microgels). The size and ζ-potential of the nanogels/microgels before and after OVA loading were measured by DLS/AccuSizer and Zetasizer, as described above. The loading capacity and loading efficiency were

determined by measuring the OVA concentration in the washing fluids with a UPLC system (Waters, USA) equipped with an Acquity BEH C4 column 1.7 µm (2.1 × 50 mm) (Waters) and a fluorescence detector (FLR, Waters). The mobile phase consisted of 0.1% TFA in 10% ACN aqueous (mobile phase A) and 0.1% TFA in 100% ACN (mobile phase B). The gradient elution was from 100% to 70% mobile phase A in 5 min. The flow rate was 0.25 mL min^{-1} and the analyses were performed at 50 ± 1 °C. The OVA calibration curve was linear between 10 and 1000 µg mL^{-1}.

In Vitro OVA Release from OVA-Loaded Dextran Nanogels: OVA-loaded nanogels were dispersed in PBS (150 × 10^{-3} M, pH 7.4) to 4 mg mL^{-1}. Glutathione was added at 8 h at a concentration of 2.5 × 10^{-3} M and again at 24 h to a final concentration of 10 × 10^{-3} M for triggered release of conjugated OVA. The release of OVA was monitored at 37 °C by taking samples at different time points, spinning down the particles (60 min, 15 000 rpm) and analyzing the supernatant for OVA concentration (see the previous paragraph).

Confocal Images of Distribution, Penetration, and Release of OVA Dextran Microgels: (a) Microgels were incubated with FITC-labeled OVA (Invirogen) for 24 h and confocal images were taken by confocal laser scanning microscopy (CLSM, Confocal Leica SPE-II, Leica Microsystems, Wetzlar, Germany). (b) FITC-labeled OVA (0.25 mg mL^{-1}, 15 µL) was added to empty dextran microgel suspensions (0.25 mg mL^{-1}, 85 µL) in 20 × 10^{-3} M HEPES buffer (pH 7.4) and immediately visualized with CLSM (1 frame/30 s) to record OVA penetration into the dextran microgels. (c) Release of FITC-OVA (nonconjugated and conjugated to the microgels) was monitored via CLSM. First, the loaded particles were dispersed in 20 × 10^{-3} M HEPES buffer (0.25 mg mL^{-1}, 100 µL); then, PBS (100 µL) and glutathione (up to a concentration of 2.5 × 10^{-3} M) were added subsequently. Confocal micrographs were taken every 30 s.

Cell Lines and Culture Conditions: D1 cells, a long-term growth factor-dependent immature myeloid dendritic cell line of splenic origin derived from a female C57BL/6 mouse, was cultured. Culture medium was IMDM (Lonza) containing 10% heat-inactivated FBS (Sigma), 2 × 10^{-3} M GlutaMax (GIBCO), 50 × 10^{-3} M β-mercaptopyridine (in IMDM), and fibroblast supernatant (SN) from NIH/3T3 cells, which was collected from confluent cultures and filtered. B3Z cells, a T-cell hybridoma expressing a T-cell receptor that specifically recognizes H-2Kb-restricted OVA MHC class I epitope SIINFEKL that carries a lacZ construct, were cultured. Culture medium was IMDM containing 10% heat-inactivated FBS, 2 × 10^{-3} M GlutaMax, 50 × 10^{-3} M β-mercaptopyridine (in IMDM).

Cytosolic Release of OVA from Nanogels: OVA-loaded nanogels were double labeled. The dextran nanogels were labeled with Alexa Fluor 488 dye (Invitrogen), whereas Alexa Fluor 647 labeled OVA (commercially available from Invitrogen) was modified with SATA and loaded in the nanogels. D1 cells were incubated with OVA-loaded

www.MaterialsViews.com

ADVANCED
FUNCTIONAL
MATERIALS
www.afm-journal.de

FULL PAPER

nanogels at a final OVA concentration of 5 μg mL^{-1} for 24 h at 37 °C. Subsequently, confocal images were taken by CLSM.

MHC Class I Antigen Presentation Assay: D1 cells (50 000 cells/well) in a 96-well plate were incubated with H-2Kb-restricted OVA class I epitope SIINFEKL, soluble OVA, soluble OVA with empty neutral nanogels, and various OVA-loaded nanogel/microgel formulations at titrated amounts of OVA for 24 h at 37 °C. Subsequently, B3Z cells (50 000 cells/well) were added to D1 cells and co-incubated with D1 cells for 24 h at 37 °C. The hybridoma B3Z cells produce β-galactosidase after being activated by DCs that present SIINFEKL, thus allowing measurement of MHC class I antigen presentation by a colorimetric assay using CPRG. β-Galactosidase activity of B3Z cells was measured by incubating the cells with 100 μL of CPRG buffer for 1 h. The β-galactosidase converted the yellow–orange substrate CPRG into the red chromophore chlorophenol red absorbing at 590 nm, and the absorbance was read by SPECTROstar (BMG Labtech, Germany).

Cytotoxicity of Nanogels/Microgels Toward D1 Cells: D1 cells (50 000 cells/well) in a 96-well plate were incubated with soluble OVA, empty neutral nanogels/microgels, and various OVA-loaded nanogel/microgel formulations at titrated amounts of OVA for 24 h at 37 °C. The relative cell viability was quantified by CellTiter 96 AQueous One Solution Cell Proliferation Assay (Promega).

Supporting Information

Supporting Information is available from the Wiley Online Library or from the author.

Acknowledgements

[1] a) T. H. Kang, A. Monie, L. S. F. Wu, X. Pang, C.-F. Hung, T. C. Wu, *Vaccine* **2011**, *29*, 1082; b) Y. Perrie, A. R. Mohammed, D. J. Kirby, S. E. McNeil, V. W. Bramwell, *Int. J. Pharm.* **2008**, *364*, 272; c) A. N. Houghton, J. S. Gold, N. E. Blachere, *Curr. Opin. Immunol.* **2001**, *13*, 134; d) M.-L. De Temmerman, J. Rejman, J. Demeester, D. J. Irvine, B. Gander, S. C. De Smedt, *Drug Discovery Today* **2011**, *16*, 569.

[2] a) M. B. Heo, Y. T. Lim, *Biomaterials* **2014**, *35*, 590; b) L. J. Thomann-Harwood, P. Kaeuper, N. Rossi, P. Milona, B. Herrmann, K. C. McCullough, *J. Controlled Release* **2013**, *166*, 95; c) A. E. Gregory, R. Titball, D. Williamson, *Front. Cell. Infect. Microbiol.* **2013**, *3*, 13; d) Z. Zhang, S. Tongchusak, Y. Mizukami, Y. J. Kang, T. Ioji, M. Touma, B. Reinhold, D. B. Keskin, E. L. Reinherz, T. Sasada, *Biomaterials* **2011**, *32*, 3666; e) S. De Koker, B. N. Lambrecht, M. A. Willart, Y. van Kooyk, J. Grooten, C. Vervaet, J. P. Remon, B. G. De Geest, *Chem. Soc. Rev.* **2011**, *40*, 320; f) B. G. De Geest, M. A. Willart, H. Hammad, B. N. Lambrecht, C. Pollard, P. Bogaert, M. De Filette, X. Saelens, C. Vervaet, J. P. Remon, J. Grooten, S. De Koker, *ACS Nano* **2012**, *6*, 2136.

[3] a) A. Pattani, V. B. Patravale, L. Panicker, P. D. Potdar, *Mol. Pharmaceutics* **2009**, *6*, 345; b) M. Dierendonck, K. Fierens, R. De Rycke, L. Lybaert, S. Maji, Z. Zhang, Q. Zhang, R. Hoogenboom, B. N. Lambrecht, J. Grooten, J. P. Remon, S. De Koker, B. G. De Geest, *Adv. Funct. Mater.* **2014**, *24*, 4634.

[4] T. Akagi, X. Wang, T. Uto, M. Baba, M. Akashi, *Biomaterials* **2007**, *28*, 3427.

[5] a) S. D. Xiang, A. Scholzen, G. Minigo, C. David, V. Apostolopoulos, P. L. Mottram, M. Plebanski, *Methods* **2006**, *40*, 1; b) V. Manolova,

A. Flace, M. Bauer, K. Schwarz, P. Saudan, M. F. Bachmann, *Eur. J. Immunol.* **2008**, *38*, 1404; c) C. Foged, B. Brodin, S. Frokjaer, A. Sundblad, *Int. J. Pharm.* **2005**, *298*, 315; d) T. Fifis, A. Gamvrellis, B. Crimeen-Irwin, G. A. Pietersz, J. Li, P. L. Mottram, I. F. McKenzie, M. Plebanski, *J. Immunol.* **2004**, *173*, 3148.

[6] V. B. Joshi, S. M. Geary, A. K. Salem, *AAPS J.* **2013**, *15*, 85.

[7] A. L. Silva, R. A. Rosalia, A. Sazak, M. G. Carstens, F. Ossendorp, J. Oostendorp, W. Jiskoot, *Eur. J. Pharm. Biopharm.* **2013**, *83*, 338.

[8] a) Y. Sasaki, K. Akiyoshi, *Chem. Rec.* **2010**, *10*, 366; b) T. Vermonden, R. Censi, W. E. Hennink, *Chem. Rev.* **2012**, *112*, 2853.

[9] C. J. Kearney, D. J. Mooney, *Nat. Mater.* **2013**, *12*, 1004.

[10] a) A. Valdebenito, P. Espinoza, E. A. Lissi, M. V. Encinas, *Polymer* **2010**, *51*, 2503; b) J. A. Cadee, M. J. van Steenbergen, C. Versluis, A. J. Heck, W. J. Underberg, W. den Otter, W. Jiskoot, W. E. Hennink, *Pharm. Res.* **2001**, *18*, 1461.

[11] X. Huang, C. S. Brazel, *J. Controlled Release* **2001**, *73*, 121.

[12] a) J. P. Schillemans, E. Verheyen, A. Barendregt, W. E. Hennink, C. F. Van Nostrum, *J. Controlled Release* **2011**, *150*, 266; b) C.-C. Lin, A. T. Metters, *Adv. Drug Delivery Rev.* **2006**, *58*, 1379.

[13] a) E. Verheyen, S. van der Wal, H. Deschout, K. Braeckmans, S. de Smedt, A. Barendregt, W. E. Hennink, C. F. van Nostrum, *J. Controlled Release* **2011**, *156*, 329; b) E. Verheyen, L. Delain-Bioton, S. van der Wal, N. el Morabit, A. Barendregt, W. E. Hennink, C. F. van Nostrum, *Macromol. Biosci.* **2010**, *10*, 1517; c) N. M. Matsumoto, D. C. Gonzalez-Toro, R. T. Chacko, H. D. Maynard, S. Thayumanavan, *Polym. Chem.* **2013**, *4*, 2464.

[14] a) A. Meister, M. E. Anderson, *Annu. Rev. Biochem.* **1983**, *52*, 711; b) D. P. Jones, J. L. Carlson, P. S. Samiec, P. Sternberg Jr., V. C. Mody Jr., R. L. Reed, L. A. S. Brown, *Clin. Chim. Acta* **1998**, *275*, 175; c) F. Meng, W. E. Hennink, Z. Zhong, *Biomaterials* **2009**, *30*, 2180; d) L. Brülisauer, M. A. Gauthier, J.-C. Leroux, *J. Controlled Release*; e) L. Brulisauer, N. Kathriner, M. Prenrecaj, M. A. Gauthier, J. C. Leroux, *Angew. Chem. Int. Ed.* **2012**, *51*, 12454.

[15] S. A. Kidwai, A. A. Ansari, A. Salahuddin, *Biochem. J.* **1976**, *155*, 171.

[16] a) W. N. E. van Dijk-Wolthuis, O. Franssen, H. Talsma, M. J. van Steenbergen, J. J. Kettenes-van den Bosch, W. E. Hennink, *Macromolecules* **1995**, *28*, 6317; b) W. N. E. van Dijk-Wolthuis, J. A. M. Hoogeboom, M. J. van Steenbergen, S. K. Y. Tsang, W. E. Hennink, *Macromolecules* **1997**, *30*, 4639; c) W. N. E. van Dijk-Wolthuis, J. J. Kettenes-van den Bosch, A. van der Kerk-van Hoof, W. E. Hennink, *Macromolecules* **1997**, *30*, 3411.

[17] J. A. Cadee, M. J. van Luyn, L. A. Brouwer, J. A. Plantinga, P. B. van Wachem, C. J. de Groot, W. den Otter, W. E. Hennink, *J. Biomed. Mater. Res.* **2000**, *50*, 397.

[18] a) X. Zhang, D. Wu, C.-C. Chu, *Biomaterials* **2004**, *25*, 4719; b) R. J. H. Stenekes, S. C. De Smedt, J. Demeester, G. Sun, Z. Zhang, W. E. Hennink, *Biomacromolecules* **2000**, *1*, 696.

[19] K. Raemdonck, B. Naeye, K. Buyens, R. E. Vandenbroucke, A. Høgset, J. Demeester, S. C. De Smedt, *Adv. Funct. Mater.* **2009**, *19*, 1406.

[20] a) Y. Ito, T. Kusawake, M. Ishida, R. Tawa, N. Shibata, K. Takada, *J. Controlled Release* **2005**, *105*, 23; b) W. Wu, Y. Wang, L. Que, *Eur. J. Pharm. Biopharm.* **2006**, *63*, 288; c) Y. Ito, H. Arai, K. Uchino, K. Iwasaki, N. Shibata, K. Takada, *Int. J. Pharm.* **2005**, *289*, 69.

[21] F. S. Steven, G. R. Tristram, *Biochem. J.* **1958**, *70*, 179.

[22] R. J. S. Duncan, P. D. Weston, R. Wrigglesworth, *Anal. Biochem.* **1983**, *132*, 68.

[23] a) O. Franssen, W. E. Hennink, *Int. J. Pharm.* **1998**, *168*, 1; b) R. J. Stenekes, O. Franssen, E. M. van Bommel, D. J. Crommelin, W. E. Hennink, *Pharm. Res.* **1998**, *15*, 557.

[24] J. Karttunen, S. Sanderson, N. Shastri, *Proc. Natl. Acad. Sci. U.S.A.* **1992**, *89*, 6020.

[25] M. T. Heemels, H. Ploegh, *Annu. Rev. Biochem.* **1995**, *64*, 463.